Protein Dynamics

DOI: 10.1002/anie.201305286

β_2-Adrenergic Receptor Activation by Agonists Studied with ^{19}F NMR Spectroscopy**

*Reto Horst, Jeffrey J. Liu, Raymond C. Stevens, and Kurt Wüthrich**

G-protein-coupled receptors (GPCRs) recognize a wide array of orthosteric ligands in their binding site on the periplasmic cell-membrane surface, initiating signal transmission through the cellular membrane to cytoplasmic partner proteins. Crystal structures of several human GPCRs in complexes with antagonists and agonists have provided insights into activation-related structural rearrangements,[1] and fluorescence spectroscopy experiments indicated activation-related conformational changes in detergent-solubilized receptors.[2] ^{19}F NMR spectroscopy and site-specific mutagenesis, as applied previously with mammalian rhodopsin,[3] more recently revealed equilibria between activated states A and inactive states I in the β_2-adrenergic receptor (β_2AR).[4] Herein, we present thermodynamic and kinetic data for these conformational equilibria in β_2AR.

In our earlier experiments,[4] the β_2AR complexes were reconstituted in mixed micelles of *n*-dodecyl-β-D-maltoside (DDM) and cholesteryl hemisuccinate (CHS), with DDM/CHS = 5:1, and ^{19}F-labels were introduced by conjugation of 2,2,2-trifluoroethanethiol (TET) with cysteine groups near the cytoplasmic ends of the helices VI (Cys265) and VII (Cys327), and at the C-terminus (Cys341). Ligand-binding assays showed that the labeled proteins retained biological activity.[4] Sequence-specific ^{19}F NMR assignments were based on comparison of β_2AR variants with single-residue TET-labeling, and the signal I was assigned from its high intensity in the apo-form of β_2AR and its complexes with inverse agonists.[4] Observation of the TET labels in β_2AR complexes with different pharmacological ligands allowed us to distinguish between the activation of two different signaling pathways.[4]

As an extension of the previous work, we analyzed the temperature dependence of the 1D ^{19}F NMR spectra of β_2AR (^{TET}C265, C327S, C341A) and β_2AR (C265A, ^{TET}C327, C341A) in terms of the thermodynamic parameters that characterize the conformational equilibria between states A and I. This analysis was focused on complexes with agonists, that is, norepinephrine and formoterol, because for the complexes with antagonists or inverse agonists the amplitude of the signal A is near the level of background noise and its height cannot be reliably quantified. Based on the observation that the temperature dependence (over the range 280–310 K) of the NMR spectra recorded with the agonist complexes was reversible, the relative populations of the conformations represented by the signals A and I, p_A and p_I,

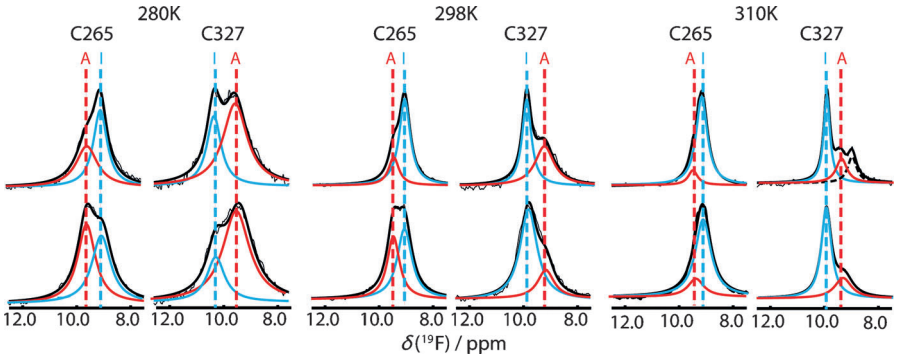

Figure 1. 1D ^{19}F NMR spectra at 280 K, 298 K, and 310 K of the complexes with the partial agonist norepinephrine (upper row) and the full agonist formoterol (lower row) of β_2AR (^{TET}C265, C327S, C341A) and β_2AR (C265A, ^{TET}C327, C341A) in mixed micelles of DDM/CHS 5:1. The ^{19}F NMR assignments are indicated at the top. The experimental spectra were deconvoluted by non-linear least-squares fits to a double-Lorentzian function. Thin and thick black lines show the experimental data and the fit function, respectively. The dotted black line in the spectrum of the norepinephine complex with β_2AR (C265A, ^{TET}C327, C341A) at 310 K represents the signal of micelle-bound free TET, which was subtracted from the experimental data before the non-linear least-squares fit was obtained for this complex. $\nu(^{19}F) = 564.8$ MHz, [β_2AR] = 25 μM, [DDM] = 1 mM, [CHS] = 0.2 mM, pH 7.5.

[*] Dr. R. Horst,[+] J. J. Liu, Prof. Dr. R. C. Stevens, Prof. Dr. K. Wüthrich
Department of Integrative Structural and Computational Biology
The Scripps Research Institute
10550 North Torrey Pines Road, La Jolla, CA 92037 (USA)
E-mail: wuthrich@scripps.edu
Prof. Dr. K. Wüthrich
Skaggs Institute for Chemical Biology
The Scripps Research Institute
10550 North Torrey Pines Road, La Jolla, CA 92037 (USA)
[+] Present address: Pfizer Worldwide Research and Development
Eastern Point Road, Groton, CT 06340 (USA)

[**] This work was supported by the NIH Roadmap initiative grant P50 GM073197 for technology development and the PSI:Biology grant U54 GM094618 for the GPCR-Network. K.W. is the Cecil H. and Ida M. Green Prof. of Structural Biology at The Scripps Research Institute. We thank Katya Kadyshevskaya for help with the illustrations.

Supporting information for this article is available on the WWW under http://dx.doi.org/10.1002/anie.201305286.

were determined by fits to a double-Lorentzian function (Figure 1), yielding an apparent equilibrium constant, $K = p_I/p_A$. $\ln K$ was found to depend linearly on the inverse of the temperature, T (Figure 2), which is in agreement with

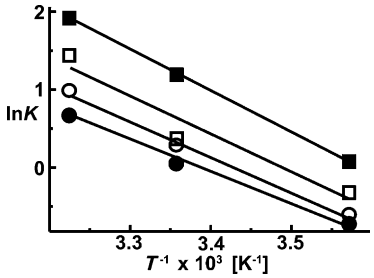

Figure 2. van't Hoff plots for the interconversion between active states (A) and inactive states (I) of β_2AR. Apparent equilibrium constants, ln*K*, were obtained from the ratios of the peak volumes of corresponding signals A and I in the ^{19}F NMR spectra of Figure 1. β_2AR (^{TET}C265, C327S, C341A) in complex with formoterol (■), β_2AR (^{TET}C265, C327S, C341A) in complex with norepinephrine (□), β_2AR (C265A, ^{TET}C327, C341A) in complex with formoterol (●), β_2AR (C265A, ^{TET}C327, C341A) in complex with norepinephrine (○). The straight lines represent linear least-squares fits of the experimental data, from which the molar enthalpy and entropy differences were obtained (Table 1).

the van't Hoff relationship (shown in Equation (1)) between K, the molar enthalpy difference, ΔH_0, and the molar entropy difference, ΔS_0.[5]

$$\ln K = -(\Delta H_0 - T S_0)/RT \quad (1)$$

where R is the gas constant. ΔH_0 values near 40 kJ mol^{-1} were obtained for both labeling sites at Cys265 and Cys327, and for both agonists used (Table 1), suggesting that the structural

Table 1: Thermodynamic parameters for the interconversion between active and inactive states of β_2AR.[a]

β_2AR complex[b]	ΔH_0 [kJ mol^{-1}]	ΔS_0 [kJ mol^{-1} K]
265/formoterol	40 ± 11	0.141 ± 0.40
265/norepinephrine	44 ± 1	0.159 ± 0.40
327/formoterol	38 ± 2	0.130 ± 0.10
327/norepinephrine	35 ± 3	0.117 ± 0.10

[a] Solubilized in DDM/CHS mixed micelles at pH 7.5. [b] 265 = β_2AR (^{TET}C265, C327S, C341A) and 327 = β_2AR (C265A, ^{TET}C327, C341A).

differences between the states A and I observed in the ^{19}F NMR spectra (Figure 1) represent more extensive conformational rearrangements than, for example, reorientation of a single amino acid side chain. For the different systems in Table 1, the Gibbs free energy, $\Delta G_0 = -\ln(K)RT$, is between zero and 3 kJ mol^{-1}, which shows that the entropy and enthalpy terms (Table 1) nearly cancel each other. This observation is in line with the widely observed entropy–enthalpy compensation in biological systems.[6]

To investigate the exchange rates between the states A and I within the framework of a two-state model (Equation (2)), where k_1 and k_{-1} are the forward and reverse rate constants,

$$A \underset{k_{-1}}{\overset{k_1}{\rightleftharpoons}} I \quad (2)$$

we used 2D ^{19}F–^{19}F exchange spectroscopy (EXSY)[7] and 1D ^{19}F saturation transfer NMR experiments.[8] The overall exchange rate constant, k_{ex}, is given by Equation (3)

$$k_{ex} = k_1 + k_{-1} = k_1/p_I = k_{-1}/p_A \quad (3)$$

where p_A and p_I are the relative populations of the states A and I. The observation of two distinct signals A and I in the ^{19}F NMR spectra of β_2AR (Figure 1) showed that the conformational exchange is slow on the ^{19}F NMR chemical-

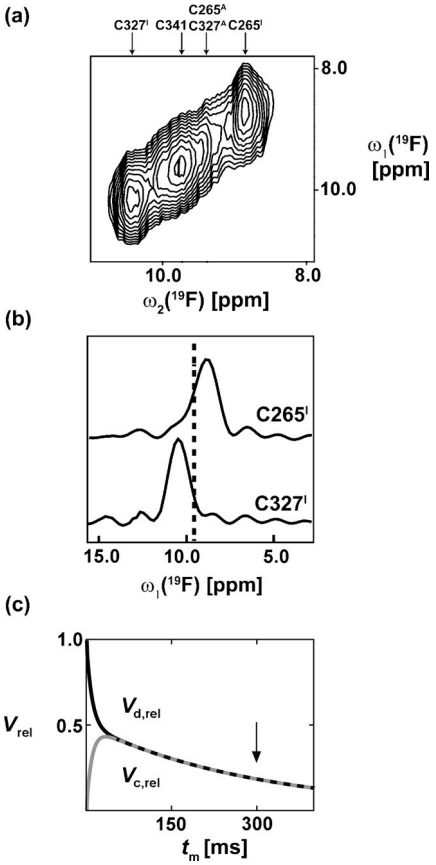

Figure 3. 2D [^{19}F,^{19}F]-EXSY experiments with the isoproterenol complex of wild type β_2AR (^{TET}C265, ^{TET}C327, ^{TET}C341) in mixed micelles of DDM/CHS 5:1. a) Contour plot: chemical shifts of five previously assigned peaks[4] are indicated (top). $\nu(^{19}F) = 564.8$ MHz, [β_2AR] = 25 μM, [DDM] = 1 mM, [CHS] = 0.2 mM, pH 7.5, $T = 280$ K. b) 1D cross-sections taken at the chemical shift positions of C265^I and C327^I. The expected positions of the cross-peaks C265^I-C265^A and C327^I-C327^A are indicated by the vertical dotted line (see text). c) Model calculation of relative NMR peak volumes, V_{rel}, at variable EXSY mixing times, t_m. V_d and V_c are the volumes of corresponding diagonal peaks and exchange cross-peaks, where $V_{d,rel} = V_d/V_o$, $V_{c,rel} = V_c/V_o$, and V_o is the diagonal peak volume at $t_m = 0$. Data were computed using $k_{ex} = 10$ s^{-1} and $T_1 = 300$ ms. Predicted values are shown for the intensities of the diagonal peaks (black line) and the cross-peaks (gray line). The arrow is at $t_m = 300$ ms, where the 2D [^{19}F,^{19}F]-EXSY spectrum shown in (a,b) was acquired.

shift time scale, so that k_{ex} satisfies the inequality (Equation (4)),

$$k_{ex} \ll \frac{\Delta\omega}{2\sqrt{p_A p_I}} \quad (4)$$

where $\Delta\omega$ is the chemical shift between I and A in rad s^{-1}.[9] For TET-labeled Cys265 and Cys327, the $\Delta\omega$ values are 2×10^3 rad s^{-1} and 4×10^3 rad s^{-1}, respectively, and $p_A = 1-p_I$ is between 0.2 and 0.9.[4] An upper limit of $k_{ex} \le 10^3$ s^{-1} was thus previously established, and additional support for this limit was obtained from experiments with paramagnetic shift reagents.[4] Herein, 2D [^{19}F,^{19}F]-EXSY experiments with a $^{TET}\beta_2$AR isoproterenol complex were performed with mixing times of 300 ms and 600 ms. For k_{ex} values of 10 s^{-1} or larger, 2D [^{19}F,^{19}F]-cross-peaks between the signals A and I are predicted to be of similar size as the diagonal peaks in these experiments (Figure 3c). The absence of [^{19}F,^{19}F]-cross-peaks (Figure 3) then enabled us to establish a new upper limit of $k_{ex} < 10$ s^{-1} at 280 K. ^{19}F NMR saturation-transfer experiments with apo-β_2AR(C265 A, ^{TET}C327, C341A) at 280 K further indicated that the exchange rate is significantly slower than 10 s^{-1}. Considering the spectral overlap of the two signals (Figure 4), we applied selective off-resonance continuous wave (cw) pre-irradiation in these experiments (Figure 4), and analyzed the resulting intensity variations of the signals A and I with model simulations based on the Bloch equations for two-site exchange (Equations (5)–(10) in the Supporting Information).[10] The longitudinal and transverse spin relaxation times, T_1 and T_2, used in these model computations were determined with an inversion-recovery experiment (see the Supporting Information) and from the line shapes of the signals in the 1D ^{19}F NMR spectrum (top trace in Figure 4), respectively. Comparison of the experimental data with the simulations (Figure 5) showed that the observed decay of the signal I was due to direct saturation by the off-resonance irradiation, and that there was no measureable contribution owing to coherence transfer from signal A to signal I by conformational exchange (Figure 5).

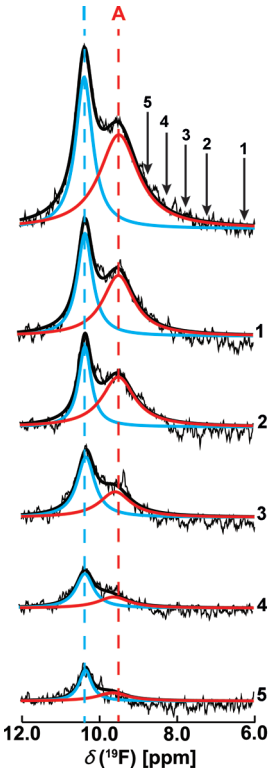

Figure 4. 1D ^{19}F NMR saturation transfer experiments with apo-β_2AR (C265A, ^{TET}C327, C341A) in mixed micelles of DDM/CHS 5:1. Top) 1D ^{19}F NMR spectrum, with peak volumes of the signals I at 10.3 ppm (cyan) and A at 9.5 ppm (red) obtained by deconvolution of the measured spectrum (thin black line) with non-linear least-squares fits of a double-Lorentzian function (thick black line). The arrows show the positions of the carrier frequency during cw pre-irradiation in the saturation transfer experiments (1)–(5), where the duration of the pre-irradiation was 500 ms and the field strength was 0.7 kHz. ν-(^{19}F) = 564.8 MHz, [β_2AR] = 25 μM, [DDM] = 1 mM, [CHS] = 0.2 mM, pH 7.5, T = 280 K.

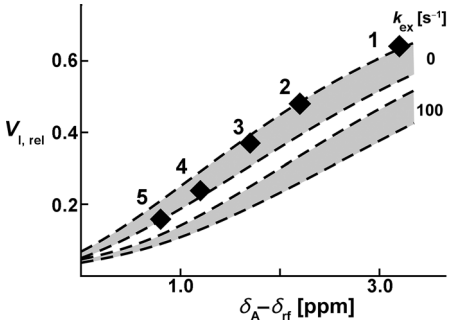

Figure 5. Model simulations of the attenuation of the intensity of signal I in the NMR spectra of Figure 4 by off-resonance cw pre-irradiation at the chemical shifts 1–5. The relative peak volumes of the signal I in 1D ^{19}F NMR saturation transfer experiments, $V_{I,rel} = V_I/V_{I,o}$, are plotted versus the frequency offset, $\delta_A-\delta_{rf}$. $V_{I,o}$ is the peak volume in the absence of pre-irradiation, and δ_A and δ_{rf} are the chemical shifts of the signal A and the carrier frequency for the cw pre-irradiation, respectively. Diamonds 1–5 are experimental data obtained from the corresponding spectra in Figure 4. The shaded areas bounded by broken lines show results of model calculations of $V_{I,rel}$ values obtained with the formalism described in the Supporting Information. Simulations were performed for two values of the rate constant in Equation (3), $k_{ex} = 0$ s^{-1} and 100 s^{-1}, and the following parameters: $p_A = 0.45$; transverse relaxation times $T_2^A = 460\pm50$ μs and $T_2^I = 810\pm80$ μs; longitudinal relaxation times $T_1^A = 300\pm40$ ms and $T_1^I = 310\pm40$ ms. The widths of the shaded areas correspond to the uncertainty in the T_1 and T_2 measurements (see text).

In conclusion, we used TET ^{19}F NMR probes attached to three cysteine residues near the cytoplasmic surface to determine thermodynamic and kinetic parameters for the equilibria between active states, A, and inactive states, I, of β_2AR, each of which represents an ensemble of rapidly interconverting conformers. Slow exchange, on the TET ^{19}F NMR chemical-shift timescale, between the states I and A enabled a quantitative characterization of this rate. Large values for ΔH_0 (Table 1) and an exchange rate slower than 10 s^{-1} (Figure 3–5) indicate that the interconversion entails major structural rearrangements, which likely involve polypeptide backbone segments.[11] Furthermore, the near-identical values of ΔH_0 for different ligands bound to the receptor (Table 1) indicate that the equilibria between A and I states are an intrinsic property of the receptor, so that binding of

different orthosteric ligands, allosteric effectors, and possibly of cytoplasmic partner proteins would result in shifts of this pre-existing equilibrium. Comparison with recent related studies of β_2AR in DDM micelles shows that TET-labeling provides different information from NMR experiments using either a different ^{19}F-label (3-bromo-1,1,1-trifluoroacetone (BTFA) on Cys 265)[12] or ^{13}C-labeled Met 82,[13] which both provided evidence for two or more states of β_2AR in fast exchange on the respective chemical-shift time scales. Results obtained by combining BTFA-labeling of Cys 265 with the use of the detergent maltose-neopentyl-glycol (MNG-3) were interpreted as manifesting slow exchange between at least three states of β_2AR that would be observable with this single ^{19}F NMR probe.[12] Different experimental approaches thus appear to provide complementary information on the β_2AR system, and studies of the dynamics of GPCRs with different reporter groups, including investigations of possible modulation of the protein conformational equilibria by allosteric effectors, are ongoing.

Received: June 19, 2013
Published online: August 16, 2013

Keywords: β_2-adrenergic receptor · ^{19}F NMR spectroscopy · G-protein-coupled receptors · protein structures

[1] a) V. Cherezov, D. M. Rosenbaum, M. A. Hanson, S. G. Rasmussen, F. S. Thian, T. S. Kobilka, H. J. Choi, P. Kuhn, W. I. Weis, B. K. Kobilka, R. C. Stevens, *Science* **2007**, *318*, 1258 – 1265; b) S. G. Rasmussen, B. T. DeVree, Y. Zou, A. C. Kruse, K. Y. Chung, T. S. Kobilka, F. S. Thian, P. S. Chae, E. Pardon, D. Calinski, J. M. Mathiesen, S. T. Shah, J. A. Lyons, M. Caffrey, S. H. Gellman, J. Steyaert, G. Skiniotis, W. I. Weis, R. K. Sunahara, B. K. Kobilka, *Nature* **2011**, *477*, 549 – 555; c) V. P. Jaakola, M. T. Griffith, M. A. Hanson, V. Cherezov, E. Y. Chien, J. R. Lane, A. P. Ijzerman, R. C. Stevens, *Science* **2008**, *322*, 1211 – 1217; d) F. Xu, H. Wu, V. Katritch, G. W. Han, K. A. Jacobson, Z. G. Gao, V. Cherezov, R. C. Stevens, *Science* **2011**, *332*, 322 – 327; e) K. Palczewski, T. Kumasaka, T. Hori, C. A. Behnke, H. Motoshima, B. A. Fox, I. Le Trong, D. C. Teller, T. Okada, R. E. Stenkamp, M. Yamamoto, M. Miyano, *Science* **2000**, *289*, 739 – 745; f) P. Scheerer, J. H. Park, P. W. Hildebrand, Y. J. Kim, N. Krauss, H. W. Choe, K. P. Hofmann, O. P. Ernst, *Nature* **2008**, *455*, 497 – 502.

[2] a) P. Ghanouni, Z. Gryczynski, J. J. Steenhuis, T. W. Lee, D. L. Farrens, J. R. Lakowicz, B. K. Kobilka, *J. Biol. Chem.* **2001**, *276*, 24433 – 24436; b) P. Ghanouni, J. J. Steenhuis, D. L. Farrens, B. K. Kobilka, *Proc. Natl. Acad. Sci. USA* **2001**, *98*, 5997 – 6002; c) U. Gether, J. A. Ballesteros, R. Seifert, E. Sanders-Bush, H. Weinstein, B. K. Kobilka, *J. Biol. Chem.* **1997**, *272*, 2587 – 2590; d) G. Swaminath, Y. Xiang, T. W. Lee, J. Steenhuis, C. Parnot, B. K. Kobilka, *J. Biol. Chem.* **2004**, *279*, 686 – 691; e) X. J. Yao, G. Velez Ruiz, M. R. Whorton, S. G. Rasmussen, B. T. DeVree, X. Deupi, R. K. Sunahara, B. Kobilka, *Proc. Natl. Acad. Sci. USA* **2009**, *106*, 9501 – 9506; f) S. Granier, S. Kim, A. M. Shafer, V. R. Ratnala, J. J. Fung, R. N. Zare, B. Kobilka, *J. Biol. Chem.* **2007**, *282*, 13895 – 13905; g) X. Yao, C. Parnot, X. Deupi, V. R. Ratnala, G. Swaminath, D. Farrens, B. Kobilka, *Nat. Chem. Biol.* **2006**, *2*, 417 – 422; h) G. Swaminath, X. Deupi, T. W. Lee, W. Zhu, F. S. Thian, T. S. Kobilka, B. Kobilka, *J. Biol. Chem.* **2005**, *280*, 22165 – 22171.

[3] a) J. Klein-Seetharaman, E. V. Getmanova, M. C. Loewen, P. J. Reeves, H. G. Khorana, *Proc. Natl. Acad. Sci. USA* **1999**, *96*, 13744 – 13749; b) M. C. Loewen, J. Klein-Seetharaman, E. V. Getmanova, P. J. Reeves, H. Schwalbe, H. G. Khorana, *Proc. Natl. Acad. Sci. USA* **2001**, *98*, 4888 – 4892.

[4] J. J. Liu, R. Horst, V. Katritch, R. C. Stevens, K. Wüthrich, *Science* **2012**, *335*, 1106 – 1110.

[5] P. W. Atkins, *Physical chemistry*, Fifth ed., Oxford University Press, Oxford, UK, **1995**, p. 285.

[6] J. D. Dunitz, *Chem. Biol.* **1995**, *2*, 709 – 712.

[7] a) J. Jeener, B. H. Meier, P. Bachmann, R. R. Ernst, *J. Chem. Phys.* **1979**, *71*, 4546 – 4553; b) B. H. Meier, R. R. Ernst, *J. Am. Chem. Soc.* **1979**, *101*, 6441 – 6442; c) H. Li, C. Frieden, *Biochemistry* **2006**, *45*, 6272 – 6278.

[8] S. Forsén, R. A. Hoffman, *J. Chem. Phys.* **1963**, *39*, 2892 – 2901.

[9] A. G. Palmer III, C. D. Kroenke, J. P. Loria, *Methods Enzymol.* **2001**, *339*, 204 – 238.

[10] a) F. Bloch, *Phys. Rev.* **1946**, *70*, 460 – 474; b) F. Bloch, W. W. Hansen, M. Packard, *Phys. Rev.* **1946**, *70*, 474 – 485; c) H. M. McConnell, *J. Chem. Phys.* **1958**, *28*, 430 – 431.

[11] D. E. Shaw, P. Maragakis, K. Lindorff-Larsen, S. Piana, R. O. Dror, M. P. Eastwood, J. A. Bank, J. M. Jumper, J. K. Salmon, Y. Shan, W. Wriggers, *Science* **2010**, *330*, 341 – 346.

[12] a) K. Y. Chung, T. H. Kim, A. Manglik, R. Alvares, B. K. Kobilka, R. S. Prosser, *J. Biol. Chem.* **2012**, *287*, 36305 – 36311; b) T. H. Kim, K. Y. Chung, A. Manglik, A. L. Hansen, R. O. Dror, T. J. Mildorf, D. E. Shaw, B. K. Kobilka, R. S. Prosser, *J. Am. Chem. Soc.* **2013**, *135*, 9465 – 9474.

[13] a) Y. Kofuku, T. Ueda, J. Okude, Y. Shiraishi, K. Kondo, M. Maeda, H. Tsujishita, I. Shimada, *Nat. Commun.* **2012**, *3*, 1045; b) R. Nygaard, Y. Zou, R. O. Dror, T. J. Mildorf, D. H. Arlow, A. Manglik, A. C. Pan, C. W. Liu, J. J. Fung, M. P. Bokoch, F. S. Thian, T. S. Kobilka, D. E. Shaw, L. Mueller, R. S. Prosser, B. K. Kobilka, *Cell* **2013**, *152*, 532 – 542.

